SUPPLEMENTARY MATERIALS

A Skin-Inspired, Capacitive Array for Tactile Modulus Detection via a Scalable Rigid-Island Architecture

Arielle Berman[1], Baiyu Shi[1], Tomasz Zaluska[2], Annika Yong[1], Sean Clees[1], Chengyi Xu[3], Levent Beker[4]*, Zhenan Bao[3]*

[1]Department of Mechanical Engineering, Stanford University, Stanford, CA 94305
[2]Department of Bioengineering, Stanford University, Stanford, CA 94305
[3]Department of Chemical Engineering, Stanford University, Stanford, CA 94305
[4]Department of Mechanical Engineering, Koç University, Rumelifeneri Yolu, Sarıyer, Istanbul, 34450, Turkey

*Corresponding author. Email: LBEKER@ku.edu.tr, zbao@stanford.edu

Supplementary Text

Discussion S1

The freestanding taxel membrane with rigid islands on either side can be modeled as a simply supported beam. We assume a distributed load since the target object contact spans the entire length of the beam. The bending stiffness can then be calculated as:

$$K = \frac{384EI}{5L^4} \quad [\mathrm{N/m^2}] \tag{S1}$$

Where E is the beam's Young's Modulus [N/m^2], L is the length of the beam [m], which is determined by the distance between the rigid islands, and I is the moment of inertia [m^4]. For a rectangular cross-section, the moment of inertia is calculated as:

$$I = \frac{bh^3}{12} \quad [\mathrm{m^4}] \tag{S2}$$

Where b is the width of the beam cross-section [m], dictated in this model as the width of the rigid island support, and h is the height of the cross-section [m], which is two-times the SEBS electrode substrate thickness.

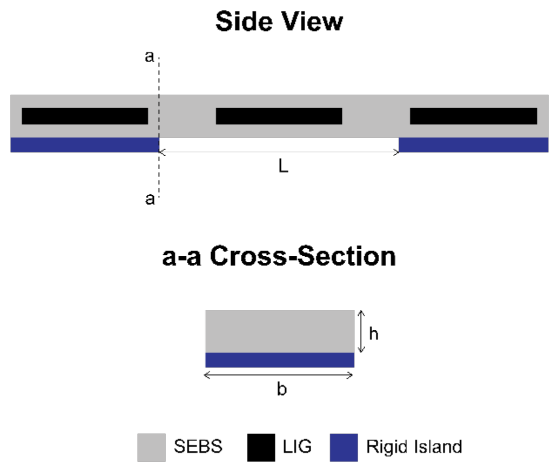

When combined, we get:

$$K = \frac{384Ebh^3}{60L^4} \quad [\mathrm{N/m^2}] \tag{S3}$$

The relationships between membrane bending stiffness and different parameters can then be used to predict impact of design changes on the capacitive output. Simply put, changes to variables that lower bending stiffness will result in greater $\overline{C_{NRI}}$ due to increased contact of the unsupported taxel with the underlying substrate, ultimately leading to decreased δ values.

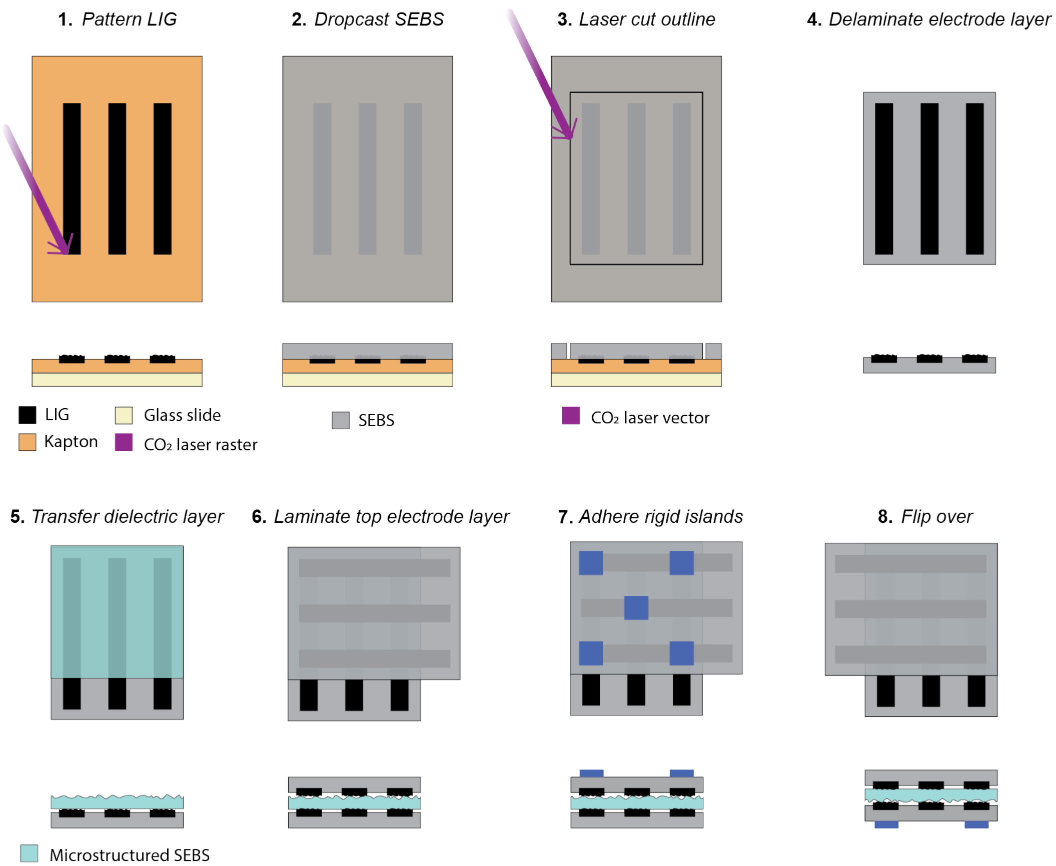

Figure S1. Modulus sensing array fabrication process.

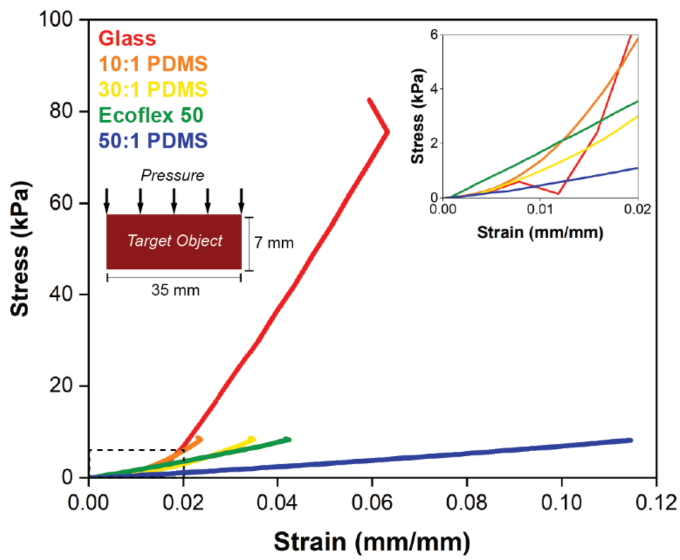

Figure S2. Experimental stress (kPa) vs. strain (mm/mm) curves of 35 mm x 35 mm x 7 mm target objects with differing moduli under increasing force to a maximum of 10 N. *Inset*: Zoomed-in data from 0 to 0.02 mm/mm strain and 0 to 6 kPa stress.

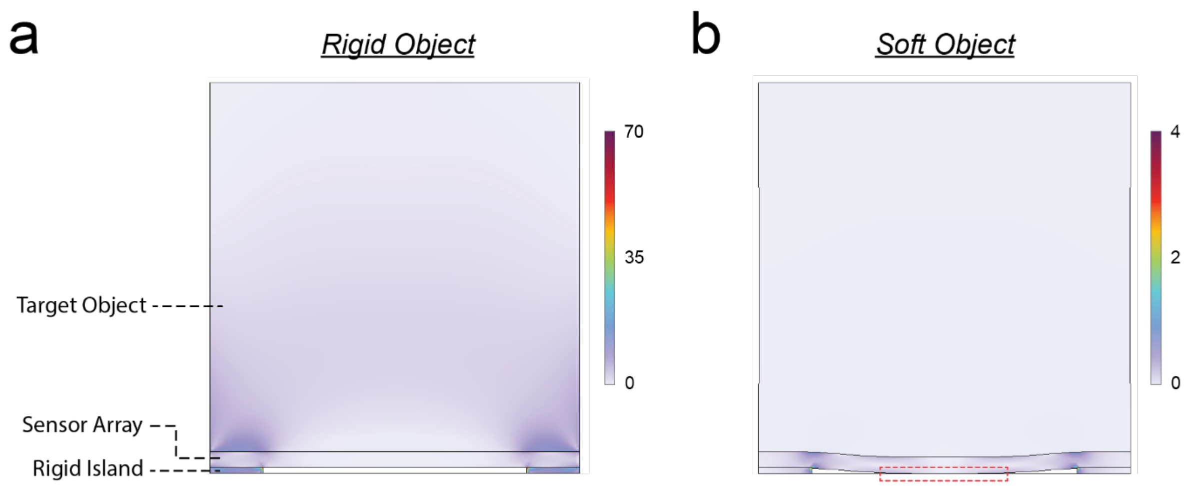

Figure S3. Simulated deformation mechanism of a sensor stack, in which the membrane is supported on either side by rigid islands, for different target object stiffnesses under 4 kPa pressure. (**a**) FEA model showing no membrane deformation when in contact with a rigid object. All stress is concentrated over the rigid islands. Color bar represents von Mises stress (N/m^2). (**b**) Simulation showing significant sensor deformation when in contact with a soft object. The red dashed box indicates the contact region between the sensor and the underlying substrate. Color bar represents von Mises stress (x 10^5 N/m^2). Both simulations use 4 kPa pressure.

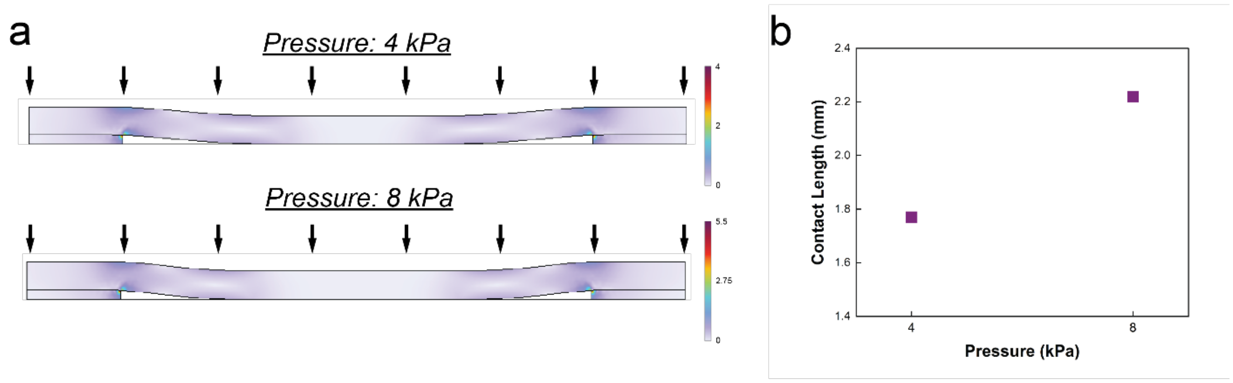

Figure S4. Simulated deformation mechanism of unsupported sensor membrane under different applied pressures applied across the entire array cross-section. (**a**) FEA results indicate that degree of membrane deformation increases as pressure grows from 4 kPa to 8 kPa. Color bar represents von Mises stress (x 10^5 N/m^2). (**b**) Calculated contact length between membrane and substrate (mm) shows positive correlation with applied pressure (kPa).

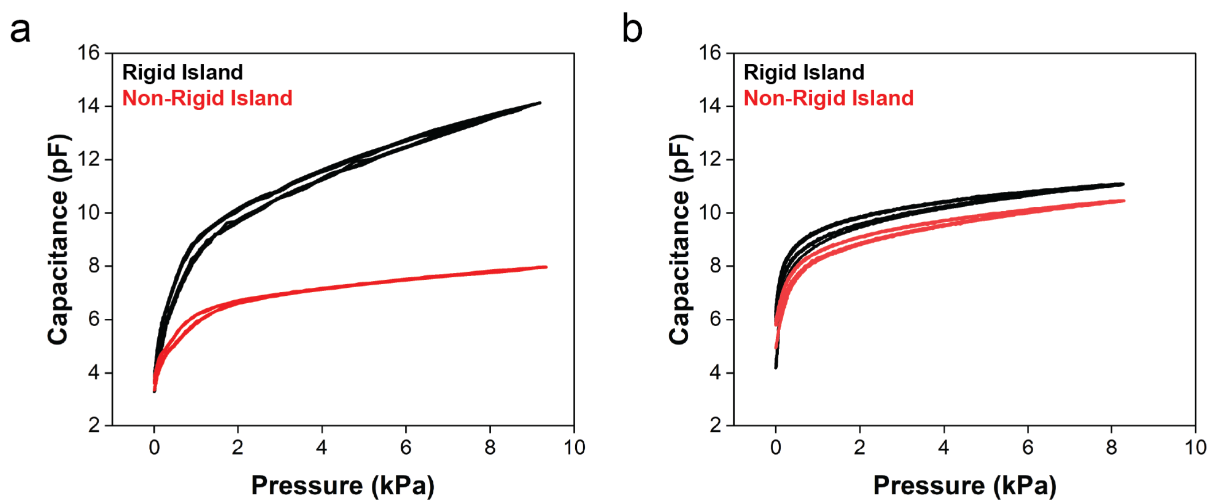

Figure S5: Capacitance (pF) vs. Pressure (kPa) under continuous loading and unloading for rigid island-supported and non-rigid island taxels. (**a**) Capacitance output of rigid and non-rigid island taxels for a 1360 kPa target object (glass). (**b**) Capacitance output of rigid and non-rigid island taxels for a 72 kPa target object (50:1 PDMS). The sensor taxels undergo 3 cycles each up to 10 N force (~8 kPa pressure).

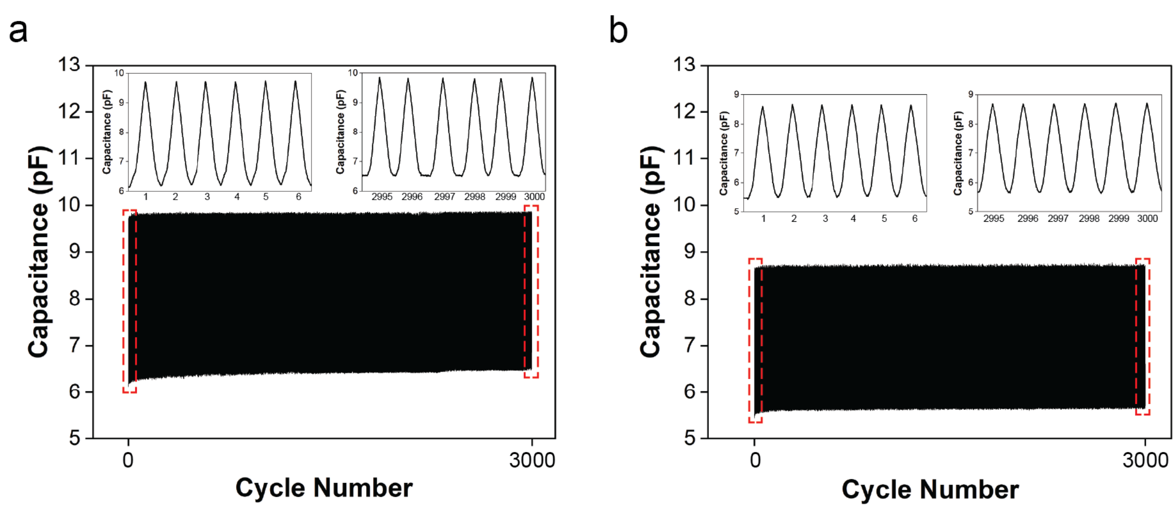

Figure S6: Cyclic loading of 3000 cycles to 10 N force (~8 kPa pressure) for a 243 kPa target object of dimensions 35 mm x 35 mm x 7 mm. (**a**) Capacitance (pF) vs. Cycle Number plot of a rigid island taxel with insets showing the first six (*left*) and the last six (*right*) cycles. (**b**) Capacitance (pF) vs. Cycle Number plot of a non-rigid island taxel with insets showing the first six (*left*) and the last six (*right*) cycles.

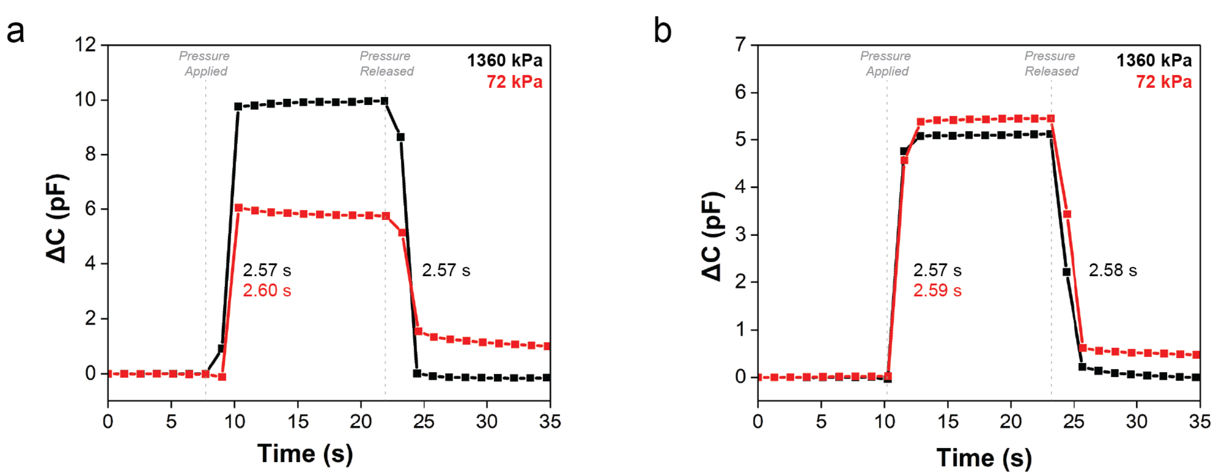

Figure S7: Taxel response and relaxation times. (**a**) Change in capacitance and corresponding response and relaxation times of rigid island taxels for a 1360 kPa target object (glass) and a 72 kPa target object (50:1 PDMS). (**b**) Change in capacitance and corresponding response and relaxation times of non-rigid island taxels for a 1360 kPa target object (glass) and a 72 kPa target object (50:1 PDMS). In both cases, 1 kg (8 kPa pressure) was applied and released.

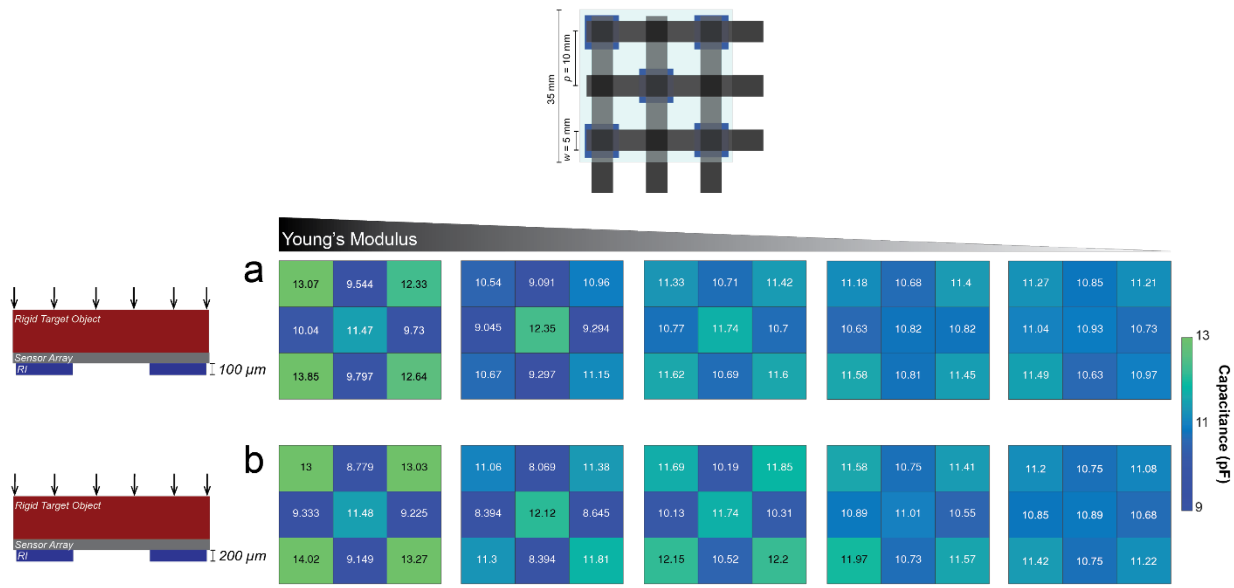

Figure S8. Comparison of capacitive outputs with different rigid island thicknesses under 8 kPa pressure. Capacitive outputs of a 3x3 array with 5 mm electrodes with (**a**) 100 µm and (**b**) 200 µm thick rigid islands. The $\overline{C_{NRI}}$ values decrease with increasing rigid island thickness.

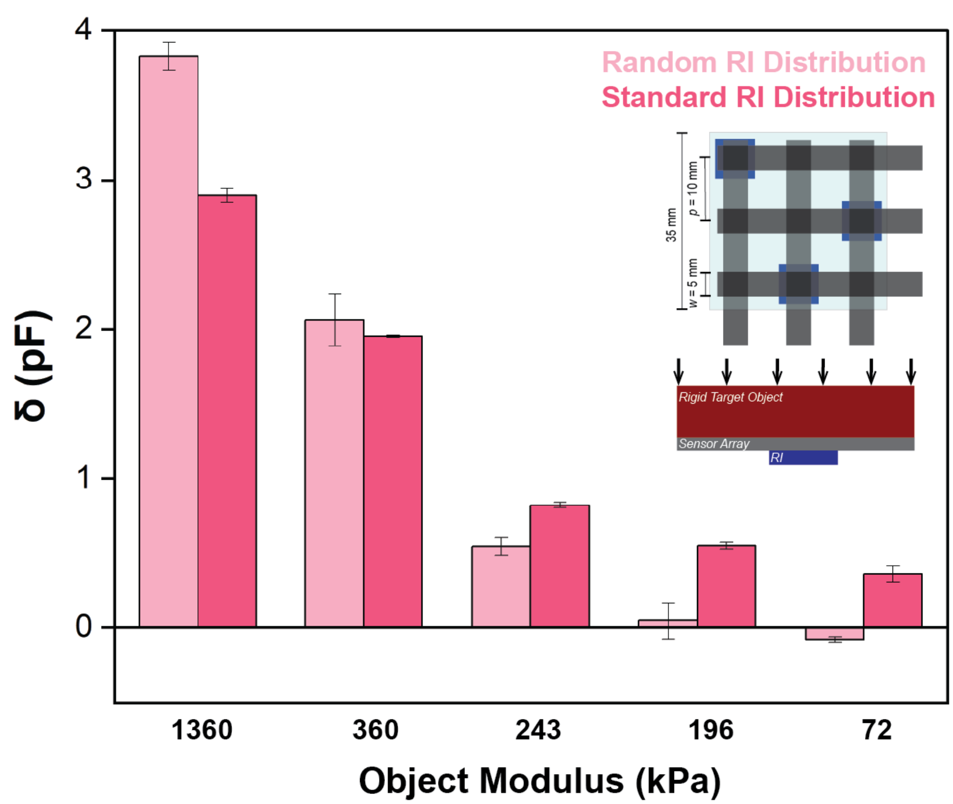

Figure S9. Bar graph comparing calibration curves under 8 kPa pressure of random rigid island distribution and standard rigid island distribution (data from Figure 1b). The inset shows the random rigid island locations and object placement.

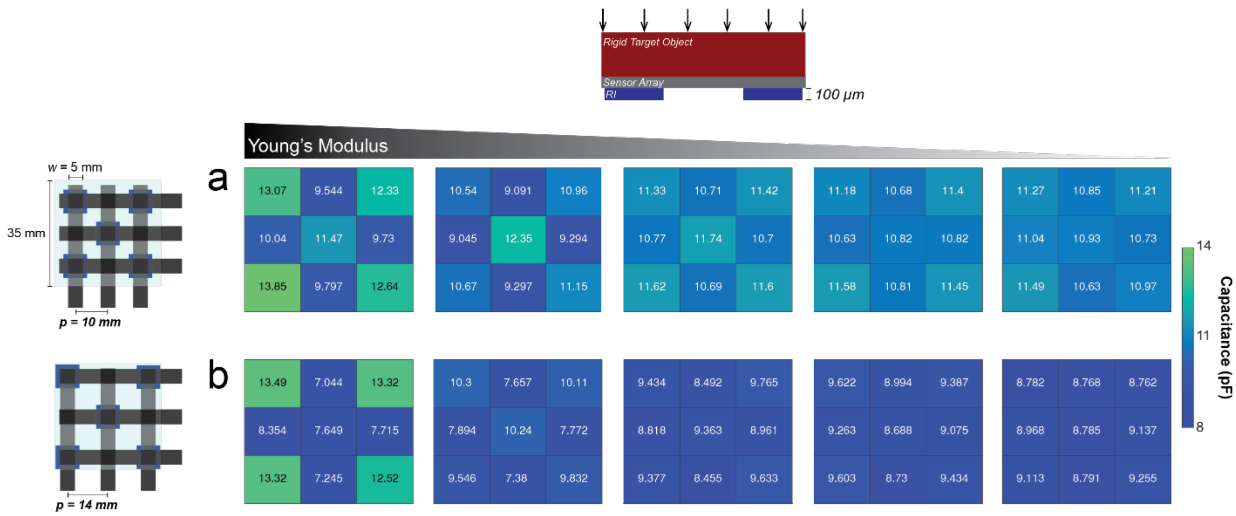

Figure S10. Effect of electrode pitch on capacitive output as a function of object modulus under 8 kPa pressure. (**a**) 10 mm pitch (**b**) 14 mm pitch. Larger pitch results in decreased difference in rigid island and non-rigid island capacitance.

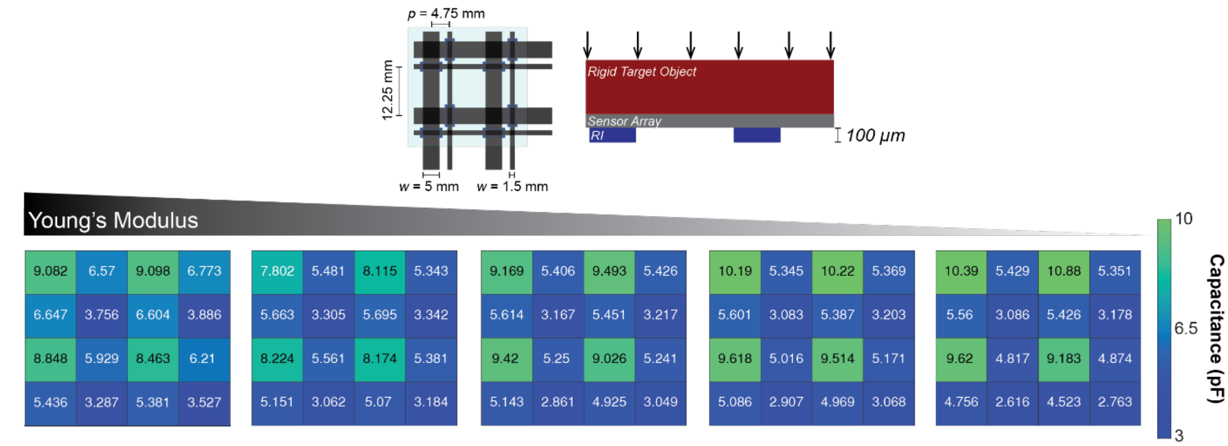

Figure S11. Visualization of higher capacitance on unsupported large taxels in array with various line widths under 8 kPa pressure.

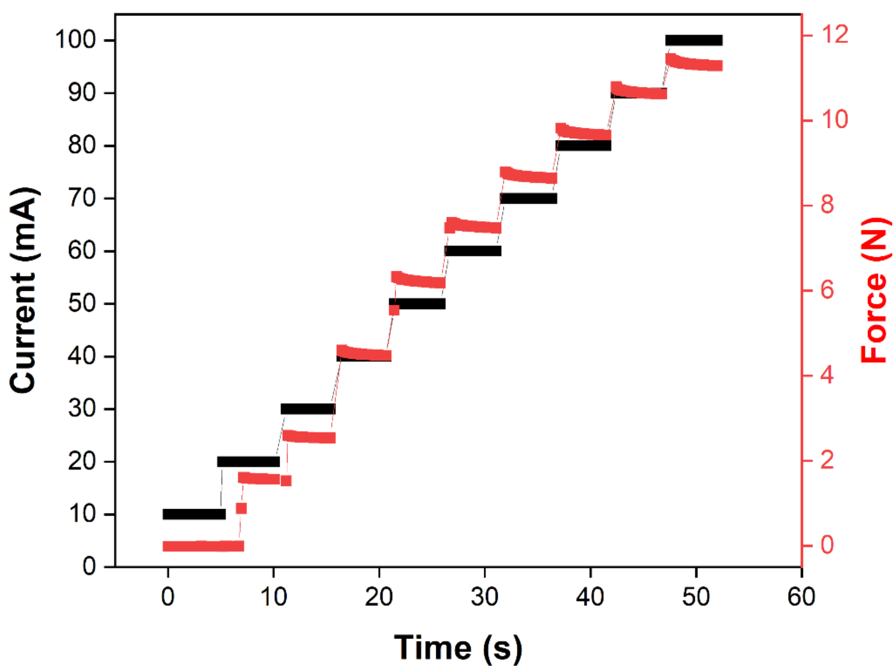

Figure S12. Plot of current (mA) supplied to servo motor and resulting force (N) applied by robotic gripper as a function of time (s). Prescribed current that increases in steps from 10 to 100 mA controls the gripper actuation, and the corresponding force (N) applied was calibrated with an external force meter as a function of time.

Table S1. Differences in capacitive outputs of arrays with different electrode widths under 8 kPa external pressure.

Electrode Width	5 mm			8 mm		
Touched Object	$\overline{C_{RI}}$	$\overline{C_{NRI}}$	**δ**	$\overline{C_{RI}}$	$\overline{C_{NRI}}$	**δ**
Glass (1360 kPa)	12.7	9.78	2.89	26.5	17.9	8.54
10:1 PDMS (360 kPa)	11.1	9.18	1.95	24.8	18.6	6.27
30:1 PDMS (243 kPa)	11.5	10.7	0.824	26.6	23.6	3.06
Ecoflex 50 (196 kPa)	11.3	10.7	0.55	25.2	23.6	1.54
50:1 PDMS (72 kPa)	11.2	10.8	0.359	26.2	25.5	0.722